JLB

Article

Rosiglitazone-induced CD36 up-regulation resolves inflammation by PPARγ and 5-LO-dependent pathways

Iván Ballesteros,[*,1] María I. Cuartero,*[*,1] Jesús M. Pradillo,*[*] Juan de la Parra,*[*] Alberto Pérez-Ruiz,*[*] Ángel Corbí,[†] Mercedes Ricote,[‡] John A. Hamilton,[§] Mónica Sobrado,[‖] José Vivancos,[‖] Florentino Nombela,[‖] Ignacio Lizasoain,*[*] and María A. Moro*[*,2]

*Unidad de Investigación Neurovascular, Departamento de Farmacología, Facultad de Medicina, Universidad Complutense, and Instituto de Investigación Hospital 12 de Octubre (i+12), Madrid, Spain; †Centro de Investigaciones Biológicas, Consejo Superior de Investigaciones Científicas, Madrid, Spain; ‡Cardiovascular Development and Repair Department, Centro Nacional de Investigaciones Cardiovasculares, Madrid, Spain; §Arthritis and Inflammation Research Centre, University of Melbourne, and Department of Medicine, Royal Melbourne Hospital, Australia; and ‖Servicio de Neurología and Instituto de Investigación Sanitaria del Hospital Universitario de La Princesa, Madrid, Spain

RECEIVED JUNE 13, 2013; REVISED NOVEMBER 11, 2013; ACCEPTED DECEMBER 1, 2013. DOI: 10.1189/jlb.0613326

ABSTRACT

PPARγ-achieved neuroprotection in experimental stroke has been explained by the inhibition of inflammatory genes, an action in which 5-LO, *Alox5*, is involved. In addition, PPARγ is known to promote the expression of CD36, a scavenger receptor that binds lipoproteins and mediates bacterial recognition and also phagocytosis. As phagocytic clearance of neutrophils is a requisite for resolution of the inflammatory response, PPARγ-induced CD36 expression might help to limit inflammatory tissue injury in stroke, an effect in which 5-LO might also be involved. Homogenates, sections, and cellular suspensions were prepared from brains of WT and *Alox5*$^{-/-}$ mice exposed to distal pMCAO. BMMs were obtained from Lys-M Cre^{+} PPARγ$^{f/f}$ and Lys-M Cre^{-} PPARγ$^{f/f}$ mice. Stereological counting of double-immunofluorescence-labeled brain sections and FACS analysis of cell suspensions was performed. In vivo and in vitro phagocytosis of neutrophils by microglia/macrophages was analyzed. PPARγ activation with RSG induced CD36 expression in resident microglia. This process was mediated by the 5-LO gene, which is induced in neurons by PPARγ activation and at least by one of its products—LXA_4—which induced CD36 independently of PPARγ. Moreover, CD36 expression helped resolution of inflammation through phagocytosis, concomitantly to neuroprotection. Based on these findings, in addition to a direct modulation by PPARγ, we propose in brain a paracrine model by which products generated by neuronal 5-LO, such as LXA_4, increase the microglial expression of CD36 and promote tissue repair in pathologies with an inflammatory component, such as stroke. *J. Leukoc. Biol.* 95: 587–598; 2014.

Introduction

The PPARγ is a nuclear transcription factor belonging to a superfamily of nuclear receptors that participate in a broad range of metabolic actions, including adipocyte differentiation and glucose homeostasis (reviewed in ref. [1]). PPARγ activation also inhibits the expression of inflammatory mediators [2–4], resulting in anti-inflammatory outcomes in several settings, including the CNS [5–7]. A prime example of this behavior is acute stroke, a devastating disease that is one of the major causes of death and disability worldwide. The neuroprotective effects of different PPARγ agonists in experimental models of stroke have been demonstrated consistently [8–12]. These effects are, at least partly, explained by the inhibition of ischemia-induced inflammation; specifically, PPARγ agonists transrepress the expression of inflammatory mediators in stroke models, such as TNF-α, iNOS, IL-1β, and MCP-1 [9, 11, 13, 14]. We demonstrated recently that the de novo expression of arachidonate 5-LO, an enzyme encoded by the *Alox5* gene, is an absolute requirement in the neuroprotective and anti-inflammatory effects of PPARγ agonists in a rat model of

Abbreviations: $^{-/-}$=knockout/deficient, 12/15-LO=12/15-lipoxygenase, Alox5/5-LO=5-lipoxygenase, BMM=bone marrow-derived macrophage, EtOH=ethyl alcohol, F=forward, GFAP=glial fibrillary acidic protein, Iba1=ionized calcium-binding adapter molecule 1, LBD=ligand-binding domain, LXA_4=lipoxin A_4, Lys-M Cre=lysozyme-M Cre, MCAO=middle cerebral artery occlusion, NDR=neutrophil decay rate, NeuN=neuronal nuclei, NIMP-R14=neutrophil marker antibody, NP-40=Nonidet P-40, PB=phosphate buffer, pMCAO=permanent middle cerebral artery occlusion, PPARγ=peroxisome proliferator-activated receptor γ, PPARγ$^{f/f}$=floxed peroxisome proliferator-activated receptor γ, R=reverse, RSG=rosiglitazone, TR-FRET=time-resolved fluorescence resonance energy transfer

The online version of this paper, found at www.jleukbio.org, includes supplemental information.

1. These authors contributed equally to this work.
2. Correspondence: Unidad de Investigación Neurovascular, Depto. de Farmacología, Facultad de Medicina, Universidad Complutense, Avda. Complutense s/n, 28040 Madrid, Spain. E-mail: neurona@med.ucm.es

stroke [15], thereby implicating proresolving mediators in signaling pathways downstream of this nuclear receptor, such as LXA_4.

There are additional effects of PPARγ that may also be highly beneficial in stroke. PPARγ has been shown to be an important regulator of the scavenger receptor CD36 [16–19], an effect with implications in multiple functions, such as uptake of oxidized LDL [18–20] and phagocytosis of apoptotic neutrophils [21–23]. As an effective elimination of neutrophils, present in the inflamed tissues, is essential for resolution of the inflammatory process [24, 25], it is plausible that the ability of PPARγ to induce the expression of this scavenger receptor actively contributes to tissue repair after stroke. Thus, with the use of an experimental murine stroke model induced by pMCAO, we studied the effect of PPARγ activation with RSG on CD36 and its contribution to resolve inflammation by increasing neutrophil phagocytosis; in addition, we explored the role of 5-LO, a gene induced early by PPARγ activation [9], and its product, LXA_4, in this process.

MATERIALS AND METHODS

Ethics statement

All of the experimental protocols were performed in accordance with the guidelines of the Animal Welfare Committee of the Universidad Complutense (EU Directives 86/609/CEE, 2003/65/CE, and 2010/63/EU).

Materials

RSG was obtained from Selleck Chemicals (Munich, Germany) or from Cayman Chemical (Ann Arbor, MI, USA). All other reagents were obtained from Sigma-Aldrich (Madrid, Spain), unless indicated otherwise.

Animals

WT controls (B6;129SF2/J) and 5-$LO^{-/-}$ mice (B6;129S2-*Alox5*^{tm1Fun}/J: *Alox5*$^{-/-}$) were obtained from The Jackson Laboratory (Bar Harbor, ME, USA), whereas the Lys-M Cre^{+} PPARγ$^{f/f}$ and Lys-M Cre^{-} PPARγ$^{f/f}$ mice were obtained as described previously [26]. All of the remaining mice were purchased from Harlan Laboratories (Indianapolis, IN, USA). The mice were housed individually in standard conditions of temperature and humidity on a 12-h light/dark cycle (lights on at 8:00 AM) and with ad libitum access to food and water.

In vivo experimental groups

Mice were assigned to the different treatment groups in a randomized fashion (based on the toss of a coin) to groups and analyzed by investigators blind to the treatments. Mice were subjected to permanent focal cerebral ischemia through a combination of distal MCAO and ipsilateral common carotid artery occlusion (pMCAO), conditions that lead to medium-sized cortical infarcts. Mice were anesthetized with 1.5–2% isoflurane in a mixture of 80% air/20% oxygen, and their body temperature was maintained at physiological levels with a heating pad throughout the surgical procedure and recovery from anesthesia.

In one set of experiments, WT and *Alox5*$^{-/-}$ mice received an i.p. injection of vehicle (saline) or RSG (3 mg/kg), 10 min after MCAO (n=6–8/group). The control animals were sham-operated animals, and they received an i.p. injection of saline or RSG, 10 min after the sham procedure. In another set of experiments, C57BL/6 mice were administered RSG or the vehicle alone in the presence or absence of the specific PPARγ antagonist T0070907 (10 mg/kg) or the 5-LO inhibitor BWA4C (5 mg/kg). Injection volumes of <0.4 ml/250 g body weight were used in all cases. Following surgery, individual animals were returned to their cages with ad libitum access to water and food. Animals were killed by an overdose of sodium pentobarbital.

No significant differences in physiological parameters were observed among the different groups studied, and no spontaneous mortality was observed after MCAO or after any of the experimental treatments.

Brain infarct determination

The infarct volume was calculated from T2-weighted images obtained by magnetic resonance analysis, using a Biospec BMT 47/40 (Bruker, Ettlingen, Germany) with ImageJ software (U.S. National Institutes of Health, Bethesda, MD, USA), or by Nissl staining, 24 h after MCAO.

Cultured cortical neurons and astrocytes

Pure cortical neuronal and astrocyte cultures were established and maintained as described previously [27].

M-CSF-cultured BMMs

BMMs were obtained by culturing bone marrow cells from the offspring of PPARγ$^{f/f}$ mice alleles and the Lys-M Cre recombinase, as described previously [26]. Bone marrow cells from Lys-M Cre^{+} PPARγ$^{f/f}$ and Lys-M Cre^{-} PPARγ$^{f/f}$ mice were resuspended in DMEM, supplemented with 10 ng/ml rM-CSF, 10% FCS, 100 U/ml penicillin, 100 μg/ml streptomycin, and 2 mM GlutaMax-1, and they were maintained for 3 days at 37°C in a humidified atmosphere of 5% CO_2. Nonadherent macrophage precursors were collected and seeded in six-well plates, and the macrophages were then cultured for 3–4 days in the presence of M-CSF (10 ng/ml) until a homogeneous population of adherent macrophages was obtained.

Western blotting

The infarct and peri-infarct areas of mouse brains were collected 24 h after MCAO, and the tissue was homogenized by sonication in the presence of protease inhibitors (Roche Diagnostics, Indianapolis, IN, USA) and 0.1% NP-40. A protein extract was prepared by high-acceleration centrifugation (12,000 g×20 min at 4°C), and 25 μg protein was denatured in Laemmli electrophoresis sample buffer (Bio-Rad, Munich, Germany) and heating at 90°C for 10 min. Proteins were separated by SDS-PAGE and transferred to a nitrocellulose membrane (Hybond-P; Amersham Biosciences Europe, Freiburg, Germany) that was probed with antibodies against CD36 (1:500; R&D Systems, Minneapolis, MN, USA). The blots were developed using ECL, and the chemiluminiscent signal was acquired with a charge-coupled device camera and quantified with GeneTools software (Syngene, Cambridge, UK). β-Actin levels were used as loading controls.

Quantitative RT-PCR

Total RNA was extracted using TRIzol reagent (Invitrogen, Carlsbad, CA, USA) from cultured macrophages, astrocytes, and neurons, treated with RSG (1 μM), LXA_4 (100 nM), or the vehicle alone (EtOH) for 5–8 h (n=3/group). The quantity of RNA was determined by spectrophotometry, and the purity was confirmed by the relative absorbance at 260 nm versus 280 nm. RNA (1 μg) was reverse-transcribed using the iScript cDNA Synthesis kit (Bio-Rad), and quantitative real-time PCR was performed in triplicate using a Bio-Rad iQ5 thermocycler. The mRNA expression was normalized to that of actin and expressed as the fold difference relative to the controls. Specific primers for rat or mouse genes were designed using Primer Express software and are as follows: 5-LO (*Rattus norvegicus*), F: 5′-GTGTCTGAGGTGTTCGGTA-3′, R: 5′-AGTGTTGATGGCAATGGT-3′; 12-LO (*R. norvegicus*), F: 5′-GGGCCACTGCAGTTCGTGA-3′, R: 5′-CGGCCTCTGCGCTCATC-3′; 15-LO (*R. norvegicus*), F: 5′-CCGGAGACTCCAAGTACGC-3′, R: 5′-CGTAGCAGCTTCCCGAGAG-3′; actin (*R. norvegicus*), F: 5′-TGAGCGCAAGTACTCTGTGTGGAT-3′, R: 5′-TAGAAGCATTTGCGGTGCACGATG-3′; CD36 (*Mus musculus*), F: 5′-TTTCCTCTGACATTTGCAGGTCTA-3′, R: 5′-AAAGGCATTGGCTGGAAGAA-3′; PPARγ (*M. musculus*), F: 5′-CACAATGCCATCAGGTTTGG-3′, R: 5′-GCTGGTCGATATCACTGGAGATC-3′; actin (*M. musculus*), F: 5′-TGTGATGGTGGGAATGGGTCAGAA-3′, R: 5′-TGTGGTGCCAGATCTTCTCCATGT-3′.

Immunofluorescence

Animals (four to six/group) were killed by pentobarbital overdose, 24 or 48 h after MCAO, and subjected to transcardiac perfusion with 0.1 M PB and 4% p-formaldehyde in 0.1 M PB (PFA, pH 7.4). Brains were removed, postfixed overnight in PFA, and placed in 30% sucrose for 48 h. Serial coronal microtome sections (30 μm; Leica SM2000R; Leica Microsystems GmbH, Wetzlar, Germany) were stored in cryoprotective solution, and dual immunofluorescence was performed on free-floating sections, incubating them overnight at 4°C with the following primary antibodies: mouse anti-mouse 5-LO (BD Biosciences, San Jose, CA, USA), rabbit anti-mouse Iba1 (Wako Pure Chemical Industries, Osaka, Japan), rabbit anti-mouse GFAP (Abcam, Cambridge, UK), rat anti-mouse NIMP-R14 (Abcam), and mouse anti-mouse NeuN (Millipore Bioscience Research Reagents, Darmstadt, Germany). Goat anti-rabbit biotin (Vector Laboratories, Burlingame, CA, USA), in combination with Alexa488 streptavidin (Molecular Probes, Eugene, OR, USA), donkey Cy3 anti-rat (Jackson ImmunoResearch, West Grove, PA, USA), and donkey Cy3 anti-mouse (Vector Laboratories), was used as a secondary antibody. Controls were performed in parallel without primary antibodies and revealed very low levels of nonspecific staining.

For 5-LO immunodetection in rat neuronal cultures, cells were treated for 24 h with vehicle (DMSO), RSG (1 μM), or RSG + T0070907 (2 μM) and then fixed with 4% PFA (15 min). The cells were then preincubated with 0.2% Triton X-100 and 10% normal goat serum in PBS for 15 min at room temperature and incubated overnight at 4°C with rabbit polyclonal antibodies against PPARγ (Santa Cruz Biotechnology, Santa Cruz, CA, USA), 5-LO (Cayman Chemical), and NeuN (Millipore Bioscience Research Reagents). The secondary antibodies used were Alexa Fluor488 anti-rabbit and Cy3 anti-mouse (1:200; Invitrogen). Cells were counterstained with TO-PRO (Invitrogen) and the controls run in parallel in the absence of primary antibodies, revealing very low levels of nonspecific staining.

Images were acquired was performed by laser-scanning confocal microscopy (LSM710; Zeiss, Munich, Germany) and analyzed with ZEN 2009 software (Zeiss). All colocalization images shown were confirmed by orthogonal projection of the z-stack files.

Brain dissociation and flow cytometry analysis

Mouse brains were removed 24 h after MCAO, and the infarct and peri-infarct tissue was dissected with a scalpel, placed into 15 mL ice-cold PBS and dissociated in a single-cell suspension, using a gentleMACS dissociator (Miltenyi Biotec, Bergisch Gladbach, Germany), according to the manufacturer's instructions. Cell suspensions were filtered through 50 μm nylon mesh strainers (BD Biosciences) and centrifuged at 300 *g* for 10 min. The pellets were resuspended in 3 mL 50% Percoll and overlaid on a 3-mL gradient of 30% Percoll, which was then centrifuged at 500 *g* for 40 min at room temperature. The cells were collected from the 30–50% interface, washed with cold PBS, and resuspended in 200 μl 2.5% BSA in PBS containing Fc blocking reagent (Miltenyi Biotec). The cell suspensions were then incubated with conjugated antibodies against CD36-allophycocyanin, Ly-6G-PerCP (BioLegend, San Diego, CA, USA), CD11b-FITC, and CD45-PE (Miltenyi Biotec) for 45 min at 4°C. Cells were washed and resuspended in 300 μl FACS Flow (BD PharMingen, San Diego, CA, USA), and isotype controls (Miltenyi Biotec) were run in parallel. Whole suspensions were analyzed on a FACSCalibur flow cytometer using CellQuest software (BD PharMingen), and data were analyzed using FlowJo software (Tree Star, Ashland, OR, USA).

Determination of LXA_4 levels

LXA_4 quantification in the cerebral cortex was performed by ELISA (EIA 45 Lipoxin A_4 assay kit; Oxford Biomedical Research, Rochester Hills, MI, USA) on tissue recovered from the MCA region, 24 h after occlusion, and in supernatants of cultured neurons and astrocytes, collected 24 h after incubation with vehicle or RSG (0.1–1 μM). The samples were first purified using C_{18} octadecyl minicolumns (Amprep mini-columns; Amersham Biosciences, Buckinghamshire, UK) and eluted with ethyl acetate, and LXA_4-containing samples were dried using an N_2 stream and redissolved in assay buffer.

Nuclear extracts

Nuclear extracts were prepared by incubating M-CSF-derived macrophages in 10 mM HEPES (pH 7.9), 1.5 mM $MgCl_2$, 10 mM KCl, and 0.5% NP-40. The nuclei were recovered by centrifugation at 12,000 *g* for 1 min at 4°C and lysed in 20 mM HEPES (pH 7.9), 15 mM $MgCl_2$, 420 mM NaCl, and 0.2 mM EDTA. After further centrifugation (12,000 *g* for 5 min at 4°C), the pellet was discarded.

In vivo phagocytosis analysis and microglial/macrophage reactivity

To analyze phagocytosis and microglial/macrophage reactivity in vivo, two photographs of the ischemic core/section were taken, using a 20× objective in seven coronal sections/animal (n=4) with a laser-scanning confocal imaging system (LSM710; Zeiss). The number of phagocytic events [28] was calculated as the number of Iba1+ cells engulfing NIMP-R14+ cells, divided by the total number of activated Iba1+ cells in the field. The double-labeled cells were quantified in the orthogonal projection of the z-stack files, using the cell-counter tool in ImageJ (NIH). Iba1 mean intensity of the converted binary image was calculated using ImageJ software.

Neutrophil quantification

To estimate the number of NIMP-R14+ in the infarct core, seven coronal sections between −1.94 and −2.46 mm, posterior to bregma (30 μm/section, 600 μm apart), were quantified with the optical fractionator approach, an unbiased cell-counting method that is not affected by the volume of reference or the size of the counted elements [29]. To calculate the NDR, we used the following formula: NDR = number of neutrophils at 48 h − number of neutrophils at 24 h.

In vitro phagocytosis assay

To assay phagocytosis in vitro, BMMs were pretreated for 12 h with RSG (1 μM), LXA_4 (100 nM), or the vehicle alone (n=4/group). Neutrophils were isolated from the C57BL/6 bone marrow cells using the neutrophil isolation kit, an LM column, and a MidiMACS separator, following the manufacturer's instructions (Miltenyi Biotec). To induce apoptosis, neutrophils were exposed to UV irradiation for 10 min and incubated in RPMI medium for 4 h at 37°C [30]. UV-induced, early apoptotic neutrophils were stained with CFSE (Invitrogen) and coincubated with macrophages for 20 min. The cells were then fixed and detached from the plate, and phagocytosis events were analyzed on a FACSCalibur flow cytometer. CFSE+ macrophages were analyzed using FlowJo software (Tree Star), and the phagocytosis index was calculated as the number of CFSE+ macrophages × mean intensity of CFSE. Less than 5% of the neutrophils used in the experiments were necrotic, as determined by PI-positive staining. CD36-PerCP (Santa Cruz Biotechnology) was used to determine CD36 expression in CFSE+ macrophages, and colocalization of F4/80+ cells (BD PharMingen) with CFSE staining was determined by confocal microscopy. For CD36 blockade, macrophages were preincubated for 1 h with a CD36-neutralizing antibody (1:500; Abcam).

TR-FRET PPARγ coactivator assay

To assess the ability of LXA_4 to act as a PPARγ ligand, in vitro TR-FRET analysis [31] was performed using the LanthaScreen TR-FRET PPARγ competitive binding assay, according to the manufacturer's instructions (Invitrogen). The robustness of the assays was determined by calculating the respective z-factors. Measurements were performed using a VICTOR 3 V multilabel counter (Wallac 1420; PerkinElmer Life and Analytical Sciences, Rodgau-Juegesheim, Germany), using the settings recommended in the LanthaScreen assay instructions.

PPARγ transcription factor activity

PPARγ transcription factor activity was assessed in nuclei obtained from M-CSF-derived macrophages. The procedure was performed using the

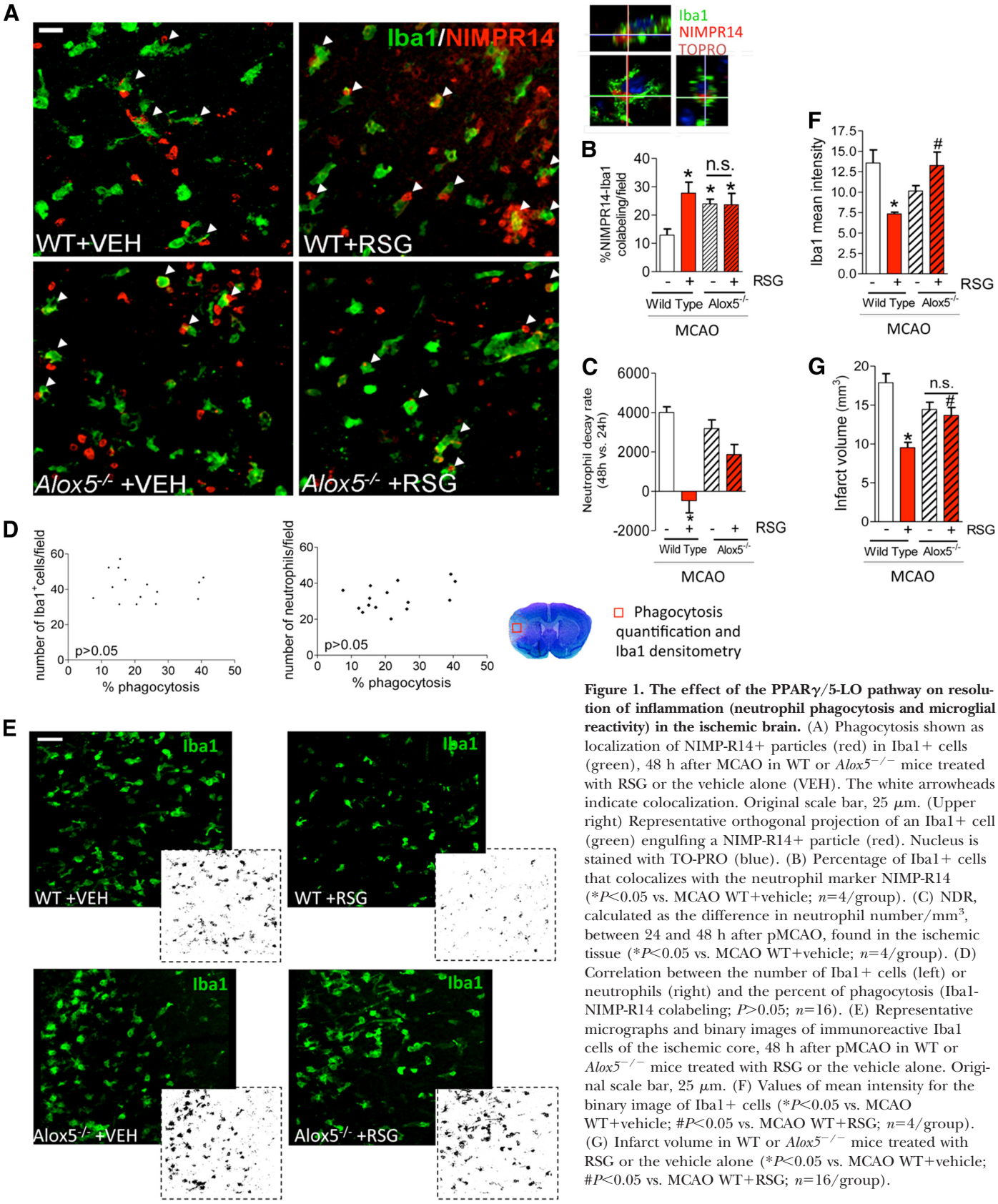

Figure 1. The effect of the PPARγ/5-LO pathway on resolution of inflammation (neutrophil phagocytosis and microglial reactivity) in the ischemic brain. (A) Phagocytosis shown as localization of NIMP-R14+ particles (red) in Iba1+ cells (green), 48 h after MCAO in WT or *Alox5*$^{-/-}$ mice treated with RSG or the vehicle alone (VEH). The white arrowheads indicate colocalization. Original scale bar, 25 μm. (Upper right) Representative orthogonal projection of an Iba1+ cell (green) engulfing a NIMP-R14+ particle (red). Nucleus is stained with TO-PRO (blue). (B) Percentage of Iba1+ cells that colocalizes with the neutrophil marker NIMP-R14 (*P<0.05 vs. MCAO WT+vehicle; n=4/group). (C) NDR, calculated as the difference in neutrophil number/mm^3, between 24 and 48 h after pMCAO, found in the ischemic tissue (*P<0.05 vs. MCAO WT+vehicle; n=4/group). (D) Correlation between the number of Iba1+ cells (left) or neutrophils (right) and the percent of phagocytosis (Iba1-NIMP-R14 colabeling; P>0.05; n=16). (E) Representative micrographs and binary images of immunoreactive Iba1 cells of the ischemic core, 48 h after pMCAO in WT or *Alox5*$^{-/-}$ mice treated with RSG or the vehicle alone. Original scale bar, 25 μm. (F) Values of mean intensity for the binary image of Iba1+ cells (*P<0.05 vs. MCAO WT+vehicle; #P<0.05 vs. MCAO WT+RSG; n=4/group). (G) Infarct volume in WT or *Alox5*$^{-/-}$ mice treated with RSG or the vehicle alone (*P<0.05 vs. MCAO WT+vehicle; #P<0.05 vs. MCAO WT+RSG; n=16/group).

PPARγ transcription factor assay kit (Cayman Chemical), following the manufacturer's recommendations.

Statistical analysis

The results are expressed as the mean ± SEM for the indicated number of experiments, and the statistical analyses were performed using Prism 4 software (GraphPad Software, La Jolla, CA, USA). Comparisons between two groups were performed using unpaired Student's *t*-tests, whereas those involving more than two groups were performed using one-way ANOVA, followed by Tukey post hoc tests. Correlation analyses were performed using Pearson's correlation. Differences were considered statistically significant at $P < 0.05$.

RESULTS

Effect of PPARγ activation with RSG on resolution of inflammation (neutrophil phagocytosis and microglial reactivity) in the ischemic brain: role of 5-LO

Activation of PPARγ may participate in neuroprotection by promoting the phagocytosis of dead cells and the subsequent resolution of inflammation. Indeed, we found that the phagocytosis of neutrophils (NIMP-R14+ cells) by microglia/macrophages (Iba1+ cells) was enhanced markedly in the brains of mice that received RSG (**Fig. 1A** and **B**; $P<0.05$ vs. MCAO WT+vehicle; $n=4$). On the other hand, the NDR, calculated as the number of neutrophils found in the ischemic hemisphere at 48 h versus that found at 24 h, was negative and significantly smaller in mice treated with RSG (Fig. 1A and C; $P<0.05$ vs. MCAO WT+vehicle; $n=4$).

These effects of RSG were not evident in the brains of *Alox5*$^{-/-}$ mice, emphasizing the crucial role of 5-LO in translating these effects of PPARγ (Fig. 1A–C; $P>0.05$; $n=4$). Interestingly, phagocytosis in untreated *Alox5*$^{-/-}$ animals, but not the NDR, was more pronounced than in its WT counterparts (Fig. 1A and B; $P<0.05$; $n=4$).

Our data also show that there is no correlation between the numbers of neutrophils or Iba1+ cells found in the sampled fields and the percent of Iba1/NIMP-R14 colabeling (Fig. 1D; $P>0.05$), thus discarding that the number of colocalization events depends on the number of individual cells in each experimental condition.

In accordance with previous reports of microglia/macrophage deactivation after phagocytosis [32], Iba1 expression in the infarcted region of RSG-treated WT animals decreased (Fig. 1E and F; $P<0.05$ vs. MCAO WT+vehicle; $P<0.05$ vs. MCAO WT+RSG; $n=4$). In contrast and despite an increased phagocytosis, microglial/macrophage reactivity in vehicle and RSG-treated *Alox5*$^{-/-}$ mice was more intense than in vehicle-treated WT mice (Fig. 1E and F; $P<0.05$; $n=4$).

As demonstrated previously [15], the PPARγ agonist RSG decreased the infarct volume, as determined 24 h after MCAO in a 5-LO-dependent fashion (Fig. 1G; $P<0.05$ vs. MCAO WT+vehicle; $P<0.05$ vs. MCAO WT+RSG; $n=16$). Moreover, the PPARγ agonist RSG reduced MCAO-induced expression of the proinflammatory molecules TNFα and MCP-1 (Supplemental Fig. 1; $P<0.05$ vs. MCAO WT+vehicle; $n=4$), as described previously [13, 33]. This anti-inflammatory effect was 5-LO-dependent (Supplemental Fig. 1; $P<0.05$ vs. MCAO WT+RSG; $n=4$), in agreement with our previous findings on rats [15]. At the time studied, RSG did not affect IL-6 levels in the ischemic brain (Supplemental Fig. 1; $P>0.05$; $n=4$); however, *Alox5*$^{-/-}$ mice, treated with RSG, presented higher levels of IL-6 in the ischemic brain than their WT counterparts (Supplemental Fig. 1; $P<0.05$ vs. MCAO WT+RSG).

The PPARγ agonist RSG induces the expression of CD36 in the ischemic brain

MCAO induced an increase in CD36 in the ipsilesional hemisphere when compared with the sham-operated group at mRNA (**Fig. 2A**; $P<0.05$; $n=4$/group) and protein levels (Fig. 2B; $P<0.05$; $n=4–8$/group). Administration of the PPARγ agonist RSG (3 mg/kg, 10 min after surgery) increased CD36 protein expression further in the ischemic brain (Fig. 2B; $P<0.05$; $n=5$). However, this increase was observed in WT but not in *Alox5*$^{-/-}$ (Fig. 2B; $P>0.05$; $n=5$).

To identify and quantify the cells that express CD36, brain tissue was analyzed by flow cytometry (**Fig. 3A**) or double-immunofluorescence staining (Fig. 3B). Our results show the presence of CD36^{+}CD11b^{+} cells in the ischemic brain, 24 h after MCAO

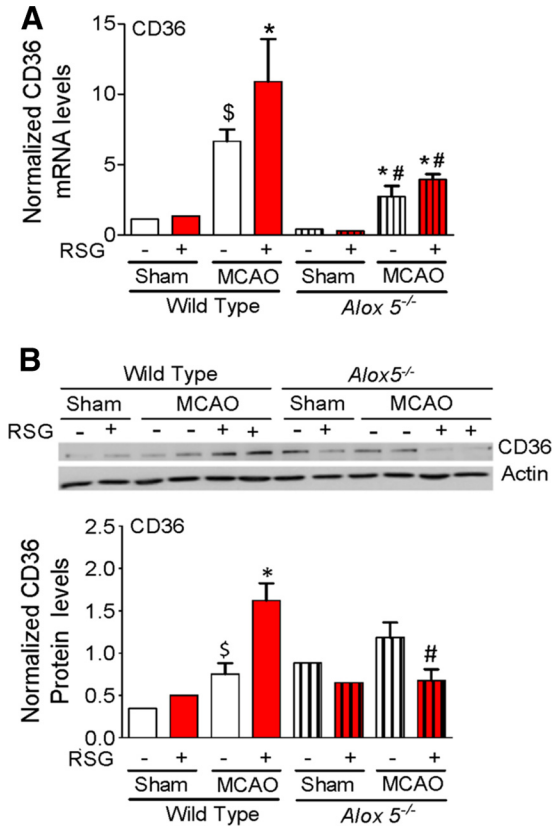

Figure 2. PPARγ agonist RSG induces 5-LO-dependent expression of CD36. (A) Expression of CD36 mRNA in the ipsilateral cortex of sham and MCAO WT or *Alox5*$^{-/-}$ mice treated with RSG or vehicle, 5 h after surgery. (B) Western blot of CD36 in homogenates of infarct and peri-infarct areas from ischemic WT or *Alox5*$^{-/-}$ mice treated with RSG or the vehicle alone, 24 h after MCAO. Expression of CD36 relative to that of actin ($\$P<0.05$ vs. sham WT; $*P<0.05$ vs. MCAO WT+vehicle; $\#P<0.05$ vs. MCAO WT+RSG; $n=5$/group).

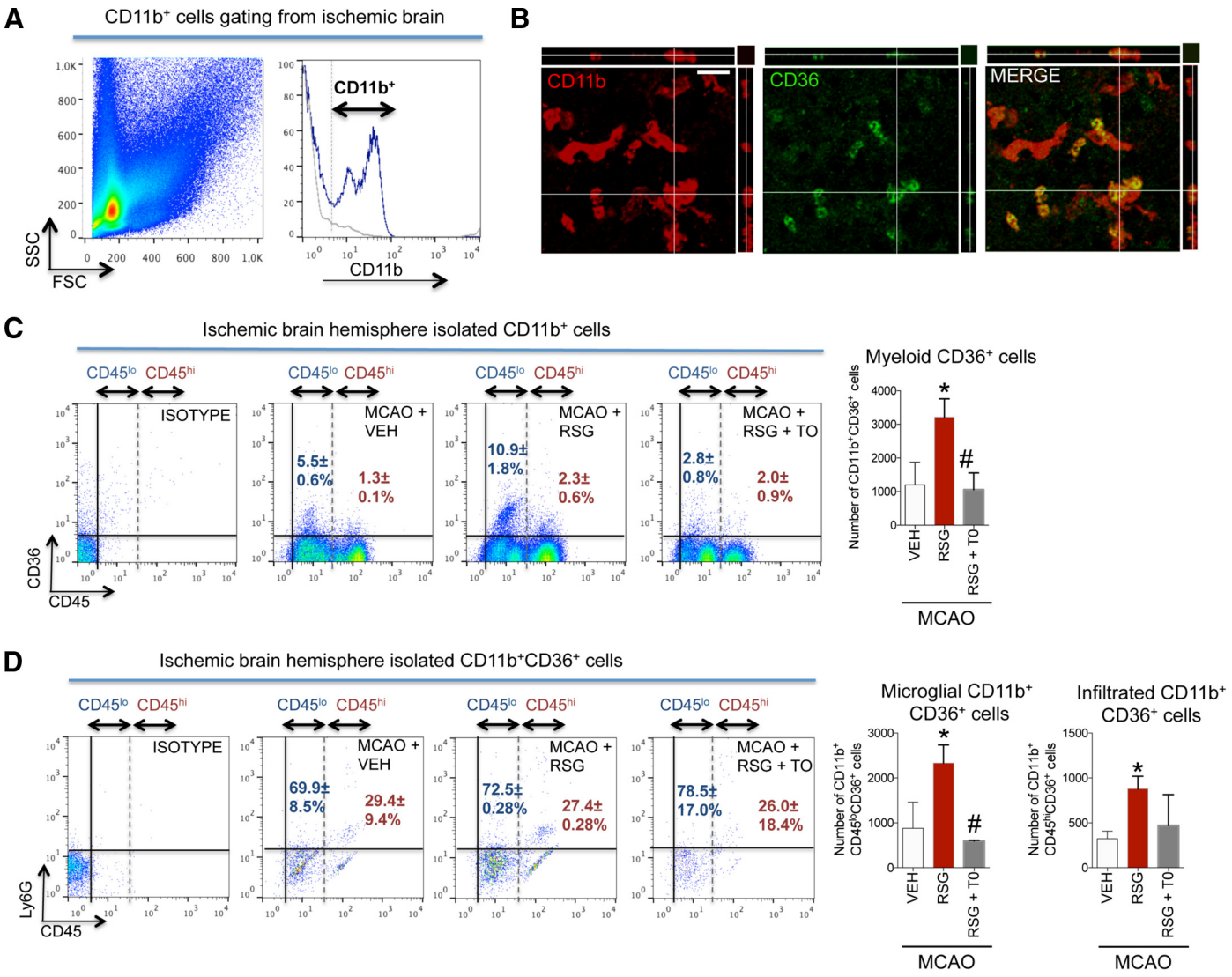

Figure 3. RSG-mediated PPARγ-dependent expression of CD36 occurs in the microglia of the ischemic tissue. (A) Representative dot plots of cells isolated from the ipsilesional hemisphere. Brain leukocyte suspensions were gated based on side-scatter (SSC) and forward-scatter (FSC) parameters (see Materials and Methods), and the $CD11b^+$ population was gated for further coexpression experiments. (B) Colocalization of CD36 (green) with the myeloid marker CD11b (red) in the core of the ischemic mouse brain, 24 h after MCAO. Original scale bar, 15 μm. (C) Representative dot plots of $CD11b^+$ brain leukocyte population, double-stained for CD45 and CD36 to identify two distinct populations, namely $CD11b^+CD45^{hi}$ (infiltrated leukocytes) and $CD11b^+CD45^{lo}$ (microglia). Cells were obtained 24 h after MCAO from mice treated with vehicle or RSG in the presence or absence of the PPARγ antagonist T0070907 (TO). The percentage of $CD36^+CD45^{lo}$ (blue) or $CD36^+CD45^{hi}$ (red) cells after each treatment is shown in the plot. The total number of $CD36^+CD11b^+$ cells found in the ischemic hemisphere is represented in the right graph (*P<0.05 vs. MCAO+vehicle; #P<0.05 vs. MCAO+RSG; n=4/group). (D) Representative dot plots of the $CD11b^+CD36^+$ brain leukocyte population double-stained for CD45 and the neutrophil marker Ly-6G. Percentages of microglial ($CD45^{lo}$) or infiltrated ($CD45^{hi}$, mostly Ly-$6G^-$) cells relative to the total $CD11b^+CD36^+$ population are shown in the plots. Right graphs represent the total number of microglial $CD36^+$ cells (left) or infiltrated $CD36^+$ cells found in the ischemic hemisphere (*P<0.05 vs. MCAO+vehicle; #P<0.05 vs. MCAO+RSG; n=4/group).

(Fig. 3B and C). Consistent with our previous findings, the treatment with RSG increased significantly the number of $CD11b^+$ cells expressing CD36 (Fig. 3C; P<0.05 vs. MCAO+vehicle; n=4). As expected, coadministration of T0070907, a specific PPARγ antagonist, reversed the RSG-induced increase in CD36-immunoreactive cells (Fig. 3C; P<0.05 vs. MCAO+RSG; n=4). In addition, treatment with the specific inhibitor of 5-LO activity, BWA4C, inhibited the RSG-mediated up-regulation of the $CD11b^+CD36^+$ cells (Supplemental Fig. 2A).

We characterized further the $CD11b^+CD36^+$ population (resident vs. infiltrates), based on the expression of CD45 (Fig. 3C and D). First, we observed that ≅70% of the $CD11b^+CD36^+$ was associated with a low expression of CD45 (Fig. 3D), corresponding to microglia ($Cd11b^+CD45^{lo}$), whereas a minor population (≅30%; Fig. 3D) displayed a higher CD45 expression, typical of infiltrates ($CD11b^+CD45^{hi}$). Moreover, coexpression analysis of CD45 with the neutrophilic marker Ly-6G showed that most of the

$CD36^+$ infiltrates were $Ly\text{-}6G^-$ (Fig. 3D), consistent with a monocytes/macrophages population of the brain. RSG increased significantly the number of $CD36^+$ microglia and $CD36^+$ myeloid infiltrates in the ischemic brain (Fig. 3D; $P<0.05$ vs. MCAO+vehicle; $n=4$), an effect that was blocked by the coadministration of the PPARγ inhibitor T0070907 in the microglial population (Fig. 3D; $P<0.05$ vs. MCAO+RSG; $n=4$). A similar effect was found in the ischemic brain of RSG-treated mice after inhibition of 5-LO activity using BWA4C (Supplemental Fig. 2; $P<0.05$ vs. MCAO+RSG; $n=4$).

The PPARγ agonist RSG augments 5-LO expression and the production of LXA_4 in the ischemic mouse brain and in rat neuronal cultures

Consistent with our previous in vivo findings in rats [15], RSG treatment also induced 5-LO expression (green) in the neurons (red) of the core and peri-infarct areas of the ischemic mice brain (**Fig. 4A** and **B**). To identify the mechanisms by which 5-LO participates in the events mediated by RSG, we quantified the amount of LXA_4, a mediator with a strong capacity to resolve inflammation and a product of 5-LO activity [34]. In this context, 5-LO up-regulation was associated with increased intracerebral LXA_4 levels, 24 h after MCAO, an effect not observed in $Alox5^{-/-}$ mice (Fig. 4C; $P<0.05$; $n=4$). These findings suggest that part of the 5-LO-dependent RSG effects could be mediated by LXA_4. Further dual immunofluorescence staining revealed that 5-LO was not expressed by $GFAP^+$ astrocytes, $Iba1^+$ microglia/macrophages, or as expected, in the $Alox5^{-/-}$ mice brain (Fig. 4D), a result that points to the neurons as crucial mediators on the RSG-induced production of intracerebral LXA_4.

Subsequently, we decided to confirm these results in in vitro cultures of rat cortical neurons, which express PPARγ (**Fig. 5A**). Our results show that RSG up-regulates 5-LO mRNA in cultured neurons (Fig. 5B; $P<0.05$ vs. vehicle; $n=4$). However, no changes were observed in 12- or 15-LO mRNA levels (Fig. 5B; $n=4$). The effect of RSG on 5-LO expression was dependent on PPARγ activity, as treatment with the specific PPARγ antagonist T0070907 abolished RSG-mediated 5-LO mRNA up-regulation (Fig. 5B; $P<0.05$ vs. RSG; $n=4$). In addition, RSG-induced 5-LO up-regulation was specific for cultured cortical neurons, as this effect was not observed in cultured astrocytes (Fig. 5C; $P<0.05$; $n=4$). This was also confirmed by immunofluorescence of 5-LO in rat cortical neurons after RSG treatment (Fig. 5D), where again, 5-LO up-regulation by RSG was lost completely when the PPARγ-specific antagonist T0070907 was included, demonstrating that neuronal 5-LO up-regulation after RSG treatment is PPARγ-dependent (Fig. 5D, bottom). In agreement, the PPARγ agonist RSG also increased LXA_4 levels in primary cultures of rat cortical neurons but not in cultured astrocytes (Fig. 5E; $P<0.05$ vs. vehicle; $n=4$).

PPARγ-induced CD36 expression is dependent on 5-LO, whereas LXA_4 induces CD36 expression independently of PPARγ in M-CSF BMMs

The increase in the levels of the 5-LO product LXA_4 observed after PPARγ activation by RSG suggests that LXA_4 may mediate signals transmitted via the PPARγ/5-LO pathway and modulate the levels of the scavenger receptor CD36 in myeloid cells. For this purpose, M-CSF BMMs were treated with the PPARγ agonist RSG, and the expression levels of PPARγ and CD36 were determined (**Fig. 6A**). First, we confirmed the presence of PPARγ mRNA expression in our M-CSF BMM cultures (Fig. 6A), which remained unchanged after treatments. Besides, we found that RSG up-regulated CD36 expression in M-CSF BMMs (Fig. 6A; $P<0.05$ vs. vehicle; $n=4$), an effect that

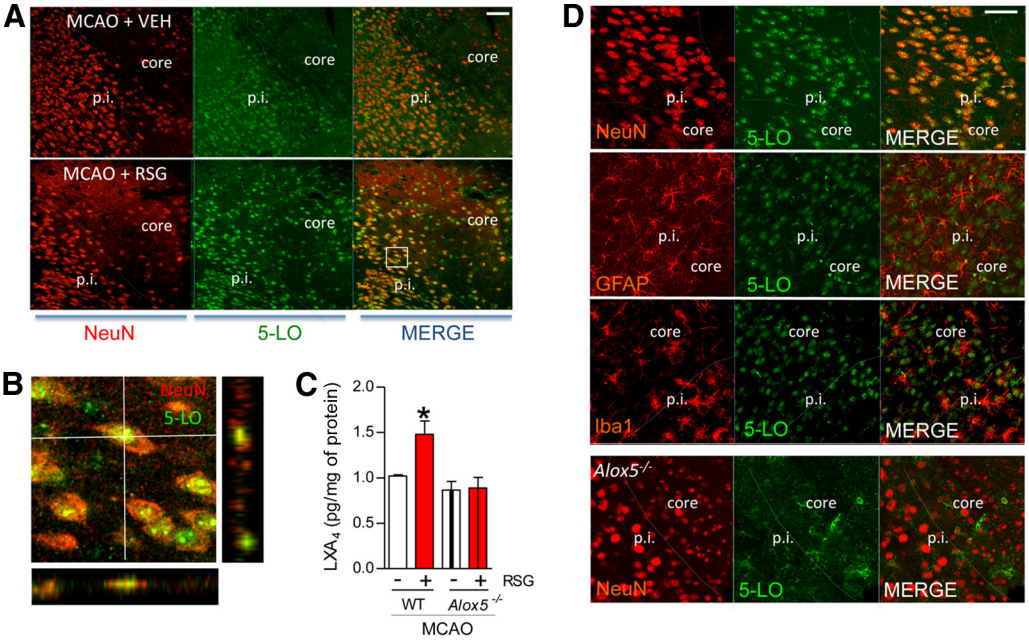

Figure 4. RSG induces the expression of 5-LO and the 5-LO-dependent synthesis of LXA_4 in the ipsilesional hemisphere of the ischemic brain. (A) Representative confocal micrographs of 5-LO (green) colocalization with the neuronal marker NeuN (red) in the peri-infarct (p.i.) and core areas of mice treated with RSG or vehicle, 24 h after MCAO. Original scale bar, 200 μm. (B) Orthogonal projection of a magnified area from a confocal micrograph from A (white square) corresponding to the peri-infarct areas of a mouse treated with RSG. (C) LXA_4 levels, 24 h after MCAO, in the ipsilesional hemisphere of WT and $Alox5^{-/-}$ mice treated with RSG or the vehicle alone (*$P<0.05$ vs. MCAO WT+vehicle; $n=4$/group). (D) Representative micrographs showing 5-LO (green) colocalization with the neuronal marker NeuN, GFAP, or Iba1 (red) in the peri-infarct areas of mice, treated with RSG or vehicle. (Bottom row) The colocalization of 5-LO (green) with NeuN (red) in the peri-infarct areas of an $Alox5^{-/-}$ mouse, 24 h after MCAO. Original scale bar, 100 μm.

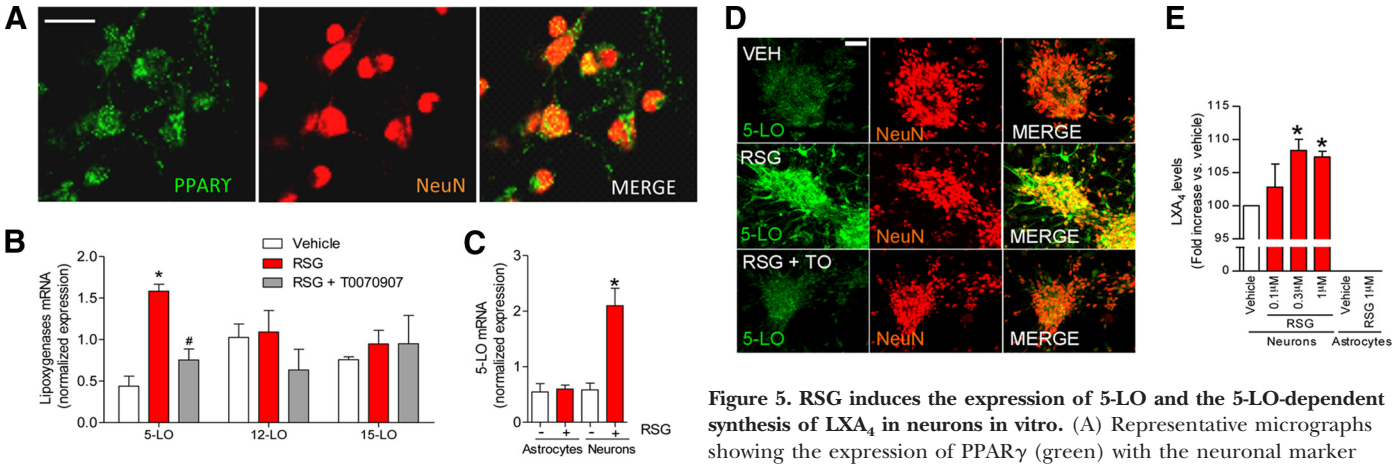

Figure 5. RSG induces the expression of 5-LO and the 5-LO-dependent synthesis of LXA_4 in neurons in vitro. (A) Representative micrographs showing the expression of PPARγ (green) with the neuronal marker NeuN (red) in the cultured rat cortical neurons used for the study. Original scale bar, 15 μm. (B) mRNA expression of lipoxygenases in cultured rat cortical neurons after treatment with vehicle, RSG, or RSG + T0070907 (*P<0.05 vs. vehicle; #P<0.05 vs. RSG; n=4/group). (C) 5-LO mRNA expression in cultured rat cortical neurons or astrocytes treated with RSG or the vehicle alone (*P<0.05 vs. vehicle; n=4/group). (D) Representative micrographs showing 5-LO (green) colocalization with the neuronal marker NeuN (red) in cultured rat cortical neurons treated with vehicle or RSG in the absence or presence of the PPARγ antagonist T0070907. Original scale bar, 50 μm. (E) LXA_4 levels in the supernatants of cultured neurons or astrocytes, treated for 24 h with RSG or the vehicle alone (*P<0.05 vs. vehicle; n=4/group).

was prevented by the 5-LO inhibitor BWA4C and by the PPARγ inhibitor T0070907 (Fig. 6A; P<0.05 vs. RSG; n=4), demonstrating that CD36 expression induced by RSG in M-CSF BMMs is PPARγ- and 5-LO-dependent. Next, we analyzed the ability of LXA_4 to induce CD36 expression in macrophages and the involvement of PPARγ in this effect. Accordingly, we used M-CSF BMMs obtained from WT and conditional PPARγ$^{-/-}$ mice with a myeloid-specific ablation of PPARγ [26], in which a clear reduction of PPARγ mRNA is observed (Fig. 6B). Our data show for the first time that LXA_4 induces the expression of CD36 in macrophages from WT mice (Fig. 6B; P<0.05 vs. vehicle; n=4) and suggest that LXA_4, at least partly, mediates the effects observed after PPARγ activation. Moreover, LXA_4, but not RSG, induced the expression of CD36 in PPARγ$^{-/-}$ BMMs, indicating that the direct effect of LXA_4 is independent of PPARγ (Fig. 6B; P<0.05 vs. vehicle; n=4). This was confirmed further by studying the ability of LXA_4 to bind the LBD of PPARγ in a TR-FRET assay [31]. Whereas RSG, a bona fide PPARγ agonist, induced FRET in a concentration-dependent manner (with an EC_{50} of 1.78 nM; Fig. 6C), LXA_4 did not bind to the PPARγ LBD in a similar assay, demonstrating that LXA_4 is not a direct PPARγ agonist. Likewise, LXA_4 failed to increase PPARγ transcription factor activity in M-CSF BMMs (Fig. 6D; P>0.05; n=5).

The role of the PPARγ/5-LO pathway and LXA_4 in phagocytosis by M-CSF BMMs and the involvement of CD36

To confirm directly the role of the PPARγ/5-LO pathway and LXA_4 in phagocytosis as a result of CD36 expression, we analyzed the phagocytosis of CFSE-labeled apoptotic neutrophils by M-CSF BMMs in vitro (**Fig. 7A–C**). RSG and LXA_4 increased CFSE intensity in macrophages after coincubation with apoptotic CFSE$^+$ neutrophils (Fig. 7A). Moreover, RSG and LXA_4 treatment increased the M-CSF BMM phagocytotic index (CFSE mean intensity×number of CFSE$^+$ macrophages; Fig. 7B and C; P<0.05 vs. vehicle; n=4–6). This effect was associated with an increased expression of CD36, determined by flow cytometry analysis of isolated M-CSF BMMs, previous to the phagocytosis assay (Fig. 7D). Notably, an anti-CD36 antibody inhibited the increase in the phagocytotic index induced by RSG and LXA_4 (Fig. 7A–C; P<0.05; n=4–6)—further evidence that RSG-mediated CD36 expression plays a role in resolving inflammation through the phagocytosis of neutrophils.

DISCUSSION

We have investigated the role of PPARγ in the resolution of inflammation after ischemic stroke. As a result, we demonstrate that PPARγ activation with RSG induces 5-LO-dependent CD36 expression in resident microglia that participates in resolution of inflammation by phagocytosis in an experimental model of stroke.

The recognition and phagocytosis of apoptotic cells by phagocytic cells, such as macrophages, are central to the successful resolution of an inflammatory response. In the case of stroke, a setting in which a potent inflammatory response has been described, pharmacological strategies able to enhance or to promote a well-orchestrated inflammation resolution could be potential therapies for this pathology. This could be the case of PPARγ agonists: our present results demonstrate that the number of neutrophils engulfed by microglia/macrophages increased in the brains of RSG-treated animals, supporting phagocytosis as a final consequence of PPARγ activity in stroke. Consistently, the rate of decay of neutrophil numbers between Days 1 and 2 was only negative in the animals treated with RSG. In addition and in agreement with previous reports of microglia deactivation after phagocytosis [32], diminished microglial reactivity was found in RSG-treated animals (Fig. 1). Moreover, RSG treatment diminished the expression of the proinflammatory markers TNF-α and MCP-1.

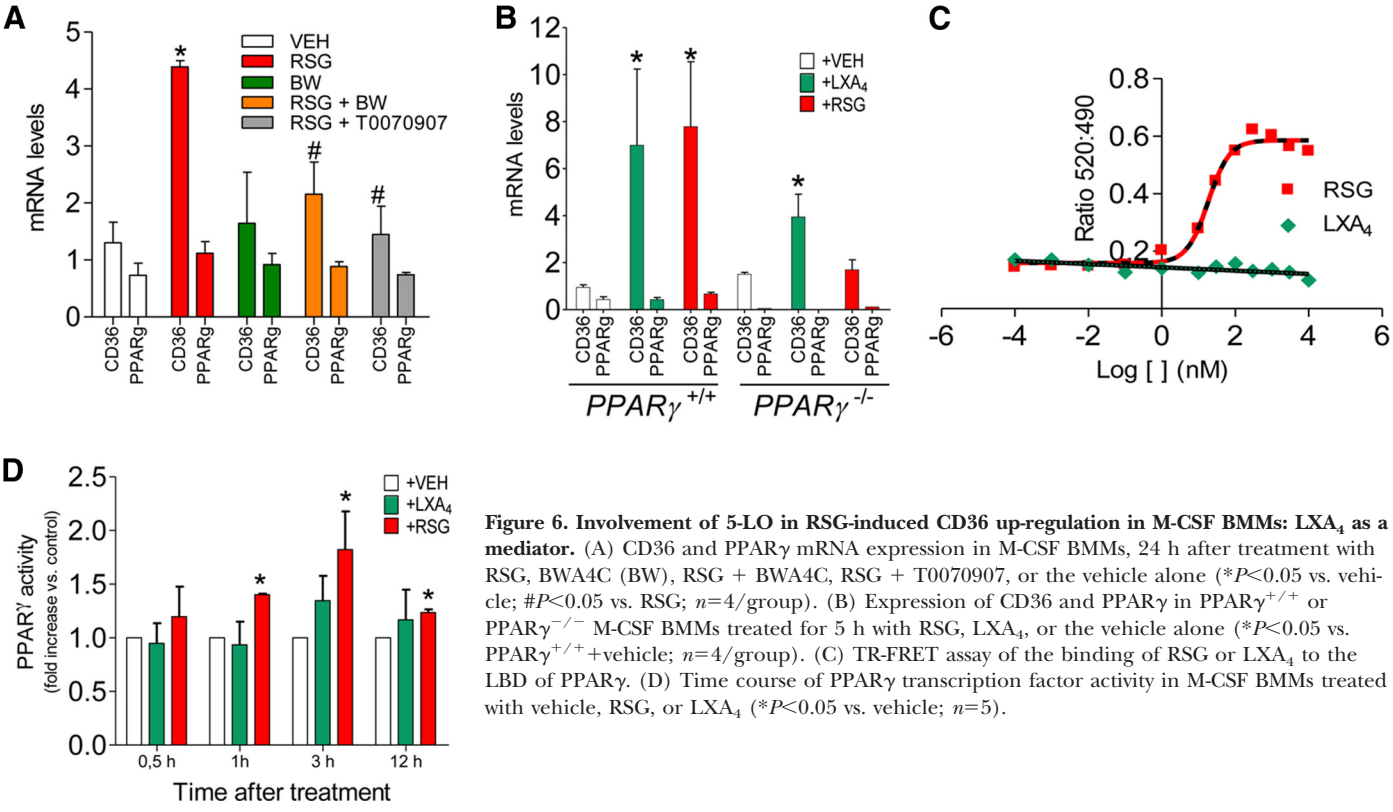

Figure 6. Involvement of 5-LO in RSG-induced CD36 up-regulation in M-CSF BMMs: LXA_4 as a mediator. (A) CD36 and PPARγ mRNA expression in M-CSF BMMs, 24 h after treatment with RSG, BWA4C (BW), RSG + BWA4C, RSG + T0070907, or the vehicle alone (*P<0.05 vs. vehicle; #P<0.05 vs. RSG; n=4/group). (B) Expression of CD36 and PPARγ in PPARγ$^{+/+}$ or PPARγ$^{-/-}$ M-CSF BMMs treated for 5 h with RSG, LXA_4, or the vehicle alone (*P<0.05 vs. PPARγ$^{+/+}$+vehicle; n=4/group). (C) TR-FRET assay of the binding of RSG or LXA_4 to the LBD of PPARγ. (D) Time course of PPARγ transcription factor activity in M-CSF BMMs treated with vehicle, RSG, or LXA_4 (*P<0.05 vs. vehicle; n=5).

Altogether, these data indicate that a PPARγ-induced increase in phagocytosis promotes resolution in the ischemic brain.

Scavenger receptors fulfill a fundamental role in phagocytosis, and CD36 is a scavenger receptor known to mediate phagocytosis of damaged, apoptotic, or senescent cells in different settings [24, 35–37]. CD36 has been claimed to be a PPARγ target gene [19]; this could therefore explain PPARγ-induced phagocytic effects. Consistently, increased phagocytosis was reported after PPARγ-induced CD36 up-regulation in different settings, including phagocytosis of apoptotic neutrophils [21, 23], malaria-parasitized erythrocytes [38], and also in the CNS [39–41]. Hence, we investigated CD36 expression in the ischemic brain and the role of PPARγ in this process. The expression of CD36 was promoted by ischemic occlusion and more importantly, increased further by the PPARγ agonist RSG, determined by immunoblotting, 24 h after MCAO (Fig. 2). Immunofluorescence analysis of the ischemic brain tissue showed that CD36$^+$ cells colocalized with the myeloid marker CD11b. In addition, the results obtained using flow cytometry analysis of brain cell suspensions (Fig. 3) clearly revealed that CD36 was expressed abundantly in the ischemic brain and that it was largely associated with CD11b$^+$CD45^{lo} cells described in the literature as microglial cells [42–44]. Moreover, RSG increased the number of myeloid cells expressing CD36 after MCAO in a PPARγ-dependent fashion. Thus, our data point to a role of CD36 up-regulation in the proresolving effects of PPARγ in stroke. These effects are likely to be performed, mainly by resident microglia and to a lesser extent, by myeloid infiltrates. In this context, CD36 up-regulation in the CNS by RSG has been linked to improved hematoma resolution [41] and β-amyloid peptide clearance in the brain [39, 40]. Although deleterious effects of CD36 have been reported [45], such effects may be counteracted in our experimental conditions by the anti-inflammatory and lipid homeostatic properties of PPARγ activation [20]. Of note, local microglial proliferation and its phagocytic activity have been shown to predominate over hematogenous macrophages in the early stages of ischemic stroke [28, 46], pointing to a relevant role for microglial CD36 up-regulation in tissue clearance and resolution of acute inflammation, at least after PPARγ activation.

We have shown previously that arachidonate 5-LO, an enzyme encoded by the *Alox5* gene, is an absolute requirement in the neuroprotective and anti-inflammatory effects of PPARγ agonists in a rat model of stroke [15]. Our present data confirm these results and demonstrate that in addition, 5-LO is involved in the proresolving actions (phagocytic events, NDR, and microglial reactivity; Fig. 1) of this nuclear receptor, as they are all absent in *Alox5*$^{-/-}$ animals. Furthermore, RSG-induced up-regulation of CD36 was not observed in the ischemic brain of 5-LO$^{-/-}$ mice or of animals treated with the 5-LO inhibitor BWA4C (Fig. 3). To the best of our knowledge, this is the first demonstration of the participation of 5-LO in PPARγ-induced CD36 expression and subsequent proresolving effects.

In agreement with our previous observation of rats, RSG also induced de novo expression of 5-LO in neurons in the mouse brain (Fig. 4). This effect was confirmed further in cultures of rat cortical neurons, where RSG mediated specifically the up-regulation of the neuronal 5-LO in a PPARγ-dependent fashion (Fig. 5). Overall, our results point to a byproduct of 5-LO metabolism as the mediator of the PPARγ/5-LO signals

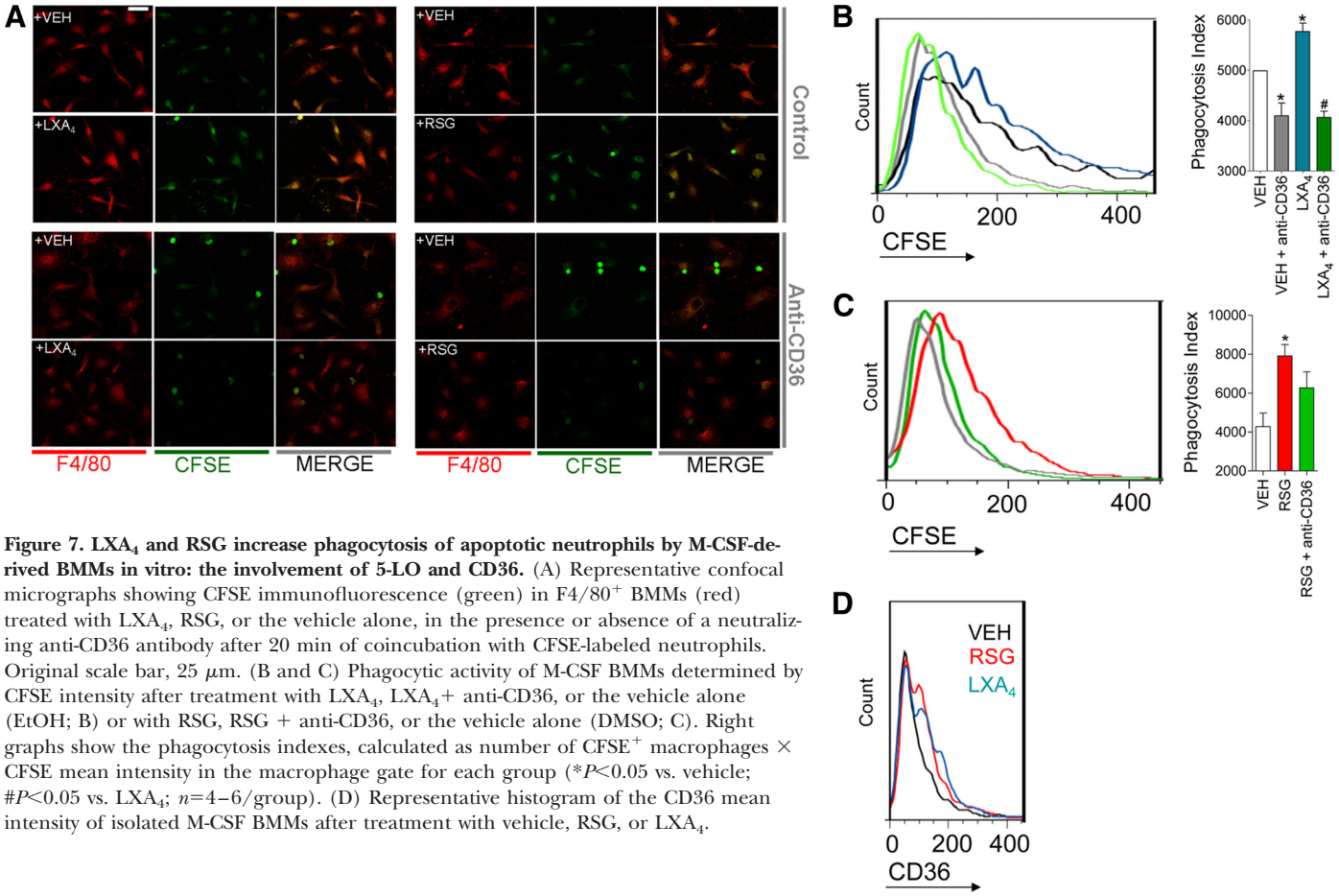

Figure 7. LXA_4 and RSG increase phagocytosis of apoptotic neutrophils by M-CSF-derived BMMs in vitro: the involvement of 5-LO and CD36. (A) Representative confocal micrographs showing CFSE immunofluorescence (green) in F4/80$^+$ BMMs (red) treated with LXA_4, RSG, or the vehicle alone, in the presence or absence of a neutralizing anti-CD36 antibody after 20 min of coincubation with CFSE-labeled neutrophils. Original scale bar, 25 μm. (B and C) Phagocytic activity of M-CSF BMMs determined by CFSE intensity after treatment with LXA_4, LXA_4+ anti-CD36, or the vehicle alone (EtOH; B) or with RSG, RSG + anti-CD36, or the vehicle alone (DMSO; C). Right graphs show the phagocytosis indexes, calculated as number of CFSE$^+$ macrophages × CFSE mean intensity in the macrophage gate for each group (*P<0.05 vs. vehicle; #P<0.05 vs. LXA_4; n=4–6/group). (D) Representative histogram of the CD36 mean intensity of isolated M-CSF BMMs after treatment with vehicle, RSG, or LXA_4.

that lead to CD36 expression and increased resolution in the ischemic brain. RSG increased the levels of the proresolving 5-LO metabolite LXA_4 in the ischemic mouse brain and in cultured rat cortical neurons but not in *Alox5*$^{-/-}$ mice or in cultured astrocytes. The PPARγ-mediated expression of 5-LO and the subsequent LXA_4 synthesis following RSG administration in our models were confined mainly to neurons, suggesting that these cells are essential control sites of PPARγ activity, at least in the ischemic brain. However, we cannot discard that apart from this paracrine action, an autocrine effect at a single cell type—microglia—might also take place.

To clarify this issue further, we studied the direct effects of LXA_4 compared with those of RSG in M-CSF BMMs (Fig. 7). These macrophages, derived of bone marrow cells cultured in M-CSF, are a frequently used and convenient population to study macrophage function and are likely to be representative of tissue macrophage populations rather than recruited "proinflammatory" macrophages [47]. Again, we show that RSG induces CD36 expression in these cells, which is dependent on 5-LO, as this effect was absent in the presence of the 5-LO inhibitor BWA4C. This experiment supports the existence of the autocrine mechanism suggested previously. In addition, our data are the first to demonstrate that LXA_4 can induce the in vitro expression of CD36 in macrophages. Furthermore, this effect of LXA_4 was independent of PPARγ, as LXA_4, but not RSG, induced the expression of CD36 in PPARγ$^{-/-}$ BMMs. Indeed, LXA_4 did not bind to the LBD of PPARγ, indicating that LXA_4 is not a direct, bona fide PPARγ agonist, nor did LXA_4 increase PPARγ transcription factor activity at the times studied in BMMs. We had suggested previously that LXA_4 could have PPARγ agonistic properties based on the study of PPARγ transcriptional activity using a heterogeneous preparation of isolated nuclei from the ischemic brain [15]. Several reasons might explain these results: in isolated brain nuclei, the balance of coactivators and corepressors of PPARγ is likely to be altered, and therefore, this preparation does not recapitulate adequately a physiological setting. In addition, we cannot discard a synergistic, indirect effect of LXA_4 of PPARγ activity in certain PPARγ$^+$ cells types—an issue that requires additional investigation.

The mechanism by which LXA_4 induces CD36 requires further study, although it may involve the activation of receptors, such as LXA_4 receptor or aryl hydrocarbon receptor [48, 49]. In this context, it has been suggested that the transcriptional activation of CD36 by PPARγ agonists is only indirectly dependent on PPARγ [50]. Now, it remains to be studied whether at least part of the induction of CD36 after PPARγ activation is directly dependent on byproducts of 5-LO, such as LXA_4.

In the absence of PPARγ activation, phagocytosis was enhanced in *Alox5*$^{-/-}$ mice, indicating that phagocytosis can also be regulated by pathways other than PPARγ/5-LO-mediated signaling. In

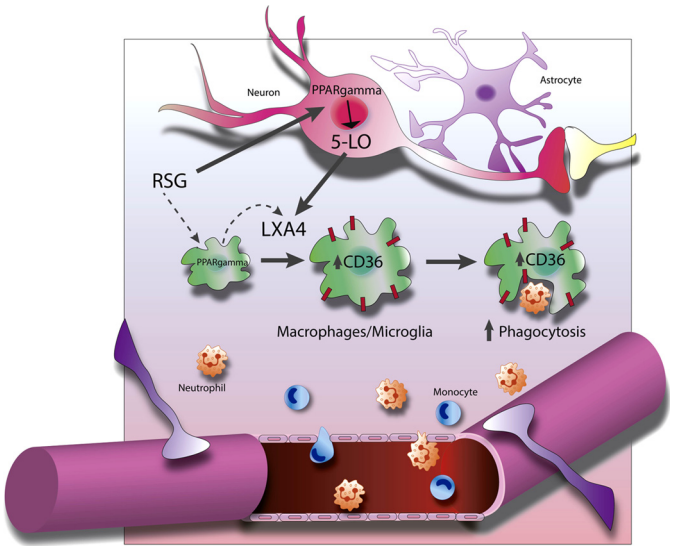

Figure 8. Schematic diagram. PPARγ activation with RSG induces 5-LO-dependent CD36 expression in resident microglia that participates in resolution of inflammation by phagocytosis in an experimental model of stroke.

this context, it has been reported that CD36 mediates a noninflammatory clearance of apoptotic cells [36, 51], in agreement with the hereby-reported anti-inflammatory properties of PPARγ agonists, which are associated mainly with resident microglial cells of the ischemic tissue. In contrast, up-regulation of phagocytosis in *Alox5*$^{-/-}$ does not seem to contribute to resolution of inflammation in ischemic stroke, as evidenced by a high Iba1 immunoreactivity and a high expression of the proinflammatory cytokine IL-6, together with a defective neutrophil clearance displayed by these mice, despite their increased phagocytic index. These results strongly suggest that loss of 5-LO activity results in an aberrant phagocytosis of apoptotic cells, in agreement with previous findings obtained after loss of 12/15-LO activity that associate lipoxygenases and by extension, lipid oxygenation to the maintenance of immune tolerance [52].

In summary (**Fig. 8**), we demonstrate that CD36 expression, induced by the PPARγ pathway, is involved in the resolution of inflammation and the subsequent clearance of infiltrated neutrophils in stroke. We also show the crucial role of the PPARγ/5-LO pathway or directly, of LXA_4: our findings suggest a paracrine model by which 5-LO products, such as LXA_4, derived from neurons of the ischemic brain after PPARγ activation, affect the phenotype of resident myeloid cells. In addition, RSG induced CD36 expression in isolated macrophages in a 5-LO-dependent manner, indicating that an autocrine model may also underlie the normal functioning of the PPARγ/5-LO pathway.

AUTHORSHIP

I.B. and M.I.C. performed surgeries, cultures, sample preparation, histological techniques, FACS, and phagocytosis assays; designed and discussed results; and helped write the manuscript. M.S. and J.d.l.P. performed surgeries. A.P-R. performed histological techniques. J.M.P., M.R., J.A.H., J.V., and F.N. designed experiments and discussed the results. A.C. and I.L. designed experiments, discussed the results, and helped write the manuscript. M.A.M. designed experiments, discussed the results, and wrote the manuscript.

ACKNOWLEDGMENTS

This work was supported by grants from the Spanish Ministry of Economy and Competitiveness CSD2010-00045 (to M.A.M.), SAF2009-08145 and SAF2012-33216 (to M.A.M.), SAF2011-23354 (to I.L.), SAF2009-07466 and SAF2012-31483 (to M.R.), from Fondo Europeo de Desarrollo Regional (FEDER) "Instituto de Salud Carlos III" RETICS RD12/0014/0003 (to I.L.) and from the local government of Madrid S2010/BMD-2336 (to M.A.M.) and S2010/BMD-2349 (to I.L.). I.B. and M.I.C. are fellows of the Spanish Ministry of Economy and Competitiveness. The authors thank Tamara Atanes and Roberto Cañadas for their technical assistance.

DISCLOSURES

The authors declare no conflict of interest.

REFERENCES

1. Kersten, S., Desvergne, B., Wahli, W. (2000) Roles of PPARs in health and disease. *Nature* **405,** 421–424.
2. Jiang, C., Ting, A. T., Seed, B. (1998) PPAR-γ agonists inhibit production of monocyte inflammatory cytokines. *Nature* **391,** 82–86.
3. Marx, N., Schonbeck, U., Lazar, M. A., Libby, P., Plutzky, J. (1998) Peroxisome proliferator-activated receptor γ activators inhibit gene expression and migration in human vascular smooth muscle cells. *Circ. Res.* **83,** 1097–1103.
4. Ricote, M., Li, A. C., Willson, T. M., Kelly, C. J., Glass, C. K. (1998) The peroxisome proliferator-activated receptor-γ is a negative regulator of macrophage activation. *Nature* **391,** 79–82.
5. Glass, C. K., Saijo, K. (2010) Nuclear receptor transrepression pathways that regulate inflammation in macrophages and T cells. *Nat. Rev. Immunol.* **10,** 365–376.
6. Landreth, G., Jiang, Q., Mandrekar, S., Heneka, M. (2008) PPARγ agonists as therapeutics for the treatment of Alzheimer's disease. *Neurotherapeutics* **5,** 481–489.
7. Tontonoz, P., Spiegelman, B. M. (2008) Fat and beyond: the diverse biology of PPARγ. *Annu. Rev. Biochem.* **77,** 289–312.
8. Pereira, M. P., Hurtado, O., Cardenas, A., Alonso-Escolano, D., Bosca, L., Vivancos, J., Nombela, F., Leza, J. C., Lorenzo, P., Lizasoain, I., Moro, M. A. (2005) The nonthiazolidinedione PPARγ agonist L-796,449 is neuroprotective in experimental stroke. *J. Neuropathol. Exp. Neurol.* **64,** 797–805.
9. Pereira, M. P., Hurtado, O., Cardenas, A., Bosca, L., Castillo, J., Davalos, A., Vivancos, J., Serena, J., Lorenzo, P., Lizasoain, I., Moro, M. A. (2006) Rosiglitazone and 15-deoxy-Δ12,14-prostaglandin J2 cause potent neuroprotection after experimental stroke through noncompletely overlapping mechanisms. *J. Cereb. Blood Flow Metab.* **26,** 218–229.
10. Shimazu, T., Inoue, I., Araki, N., Asano, Y., Sawada, M., Furuya, D., Nagoya, H., Greenberg, J. H. (2005) A peroxisome proliferator-activated receptor-γ agonist reduces infarct size in transient but not in permanent ischemia. *Stroke* **36,** 353–359.
11. Sundararajan, S., Gamboa, J. L., Victor, N. A., Wanderi, E. W., Lust, W. D., Landreth, G. E. (2005) Peroxisome proliferator-activated receptor-γ ligands reduce inflammation and infarction size in transient focal ischemia. *Neuroscience* **130,** 685–696.
12. Zhao, Y., Patzer, A., Herdegen, T., Gohlke, P., Culman, J. (2006) Activation of cerebral peroxisome proliferator-activated receptors γ promotes neuroprotection by attenuation of neuronal cyclooxygenase-2 overexpression after focal cerebral ischemia in rats. *FASEB J.* **20,** 1162–1175.
13. Luo, Y., Yin, W., Signore, A. P., Zhang, F., Hong, Z., Wang, S., Graham, S. H., Chen, J. (2006) Neuroprotection against focal ischemic brain injury by the peroxisome proliferator-activated receptor-γ agonist rosiglitazone. *J. Neurochem.* **97,** 435–448.
14. Tureyen, K., Kapadia, R., Bowen, K. K., Satriotomo, I., Liang, J., Feinstein, D. L., Vemuganti, R. (2007) Peroxisome proliferator-activated receptor-γ agonists induce neuroprotection following transient focal ischemia in normotensive, normoglycemic as well as hypertensive and type-2 diabetic rodents. *J. Neurochem.* **101,** 41–56.
15. Sobrado, M., Pereira, M. P., Ballesteros, I., Hurtado, O., Fernandez-Lopez, D., Pradillo, J. M., Caso, J. R., Vivancos, J., Nombela, F., Serena, J.,

Lizasoain, I., Moro, M. A. (2009) Synthesis of lipoxin A4 by 5-lipoxygenase mediates PPARγ-dependent, neuroprotective effects of rosiglitazone in experimental stroke. *J. Neurosci.* **29,** 3875–3884.
16. Chawla, A., Barak, Y., Nagy, L., Liao, D., Tontonoz, P., Evans, R. M. (2001) PPAR-γ dependent and independent effects on macrophage-gene expression in lipid metabolism and inflammation. *Nat. Med.* **7,** 48–52.
17. Motojima, K., Passilly, P., Peters, J. M., Gonzalez, F. J., Latruffe, N. (1998) Expression of putative fatty acid transporter genes are regulated by peroxisome proliferator-activated receptor α and γ activators in a tissue- and inducer-specific manner. *J. Biol. Chem.* **273,** 16710–16714.
18. Nagy, L., Tontonoz, P., Alvarez, J. G., Chen, H., Evans, R. M. (1998) Oxidized LDL regulates macrophage gene expression through ligand activation of PPARγ. *Cell* **93,** 229–240.
19. Tontonoz, P., Nagy, L., Alvarez, J. G., Thomazy, V. A., Evans, R. M. (1998) PPARγ promotes monocyte/macrophage differentiation and uptake of oxidized LDL. *Cell* **93,** 241–252.
20. Moore, K. J., Rosen, E. D., Fitzgerald, M. L., Randow, F., Andersson, L. P., Altshuler, D., Milstone, D. S., Mortensen, R. M., Spiegelman, B. M., Freeman, M. W. (2001) The role of PPAR-γ in macrophage differentiation and cholesterol uptake. *Nat. Med.* **7,** 41–47.
21. Asada, K., Sasaki, S., Suda, T., Chida, K., Nakamura, H. (2004) Antiinflammatory roles of peroxisome proliferator-activated receptor γ in human alveolar macrophages. *Am. J. Respir. Crit. Care Med.* **169,** 195–200.
22. Greenberg, M. E., Sun, M., Zhang, R., Febbraio, M., Silverstein, R., Hazen, S. L. (2006) Oxidized phosphatidylserine-CD36 interactions play an essential role in macrophage-dependent phagocytosis of apoptotic cells. *J. Exp. Med.* **203,** 2613–2625.
23. Shimizu, K., Kobayashi, M., Tahara, J., Shiratori, K. (2005) Cytokines and peroxisome proliferator-activated receptor γ ligand regulate phagocytosis by pancreatic stellate cells. *Gastroenterology* **128,** 2105–2118.
24. Savill, J. (1997) Apoptosis in resolution of inflammation. *J. Leukoc. Biol.* **61,** 375–380.
25. Serhan, C. N., Savill, J. (2005) Resolution of inflammation: the beginning programs the end. *Nat. Immunol.* **6,** 1191–1197.
26. Roszer, T., Menendez-Gutierrez, M. P., Lefterova, M. I., Alameda, D., Nunez, V., Lazar, M. A., Fischer, T., Ricote, M. (2011) Autoimmune kidney disease and impaired engulfment of apoptotic cells in mice with macrophage peroxisome proliferator-activated receptor γ or retinoid X receptor α deficiency. *J. Immunol.* **186,** 621–631.
27. Romera, C., Hurtado, O., Botella, S. H., Lizasoain, I., Cardenas, A., Fernandez-Tome, P., Leza, J. C., Lorenzo, P., Moro, M. A. (2004) In vitro ischemic tolerance involves upregulation of glutamate transport partly mediated by the TACE/ADAM17-tumor necrosis factor-α pathway. *J. Neurosci.* **24,** 1350–1357.
28. Denes, A., Vidyasagar, R., Feng, J., Narvainen, J., McColl, B. W., Kauppinen, R. A., Allan, S. M. (2007) Proliferating resident microglia after focal cerebral ischaemia in mice. *J. Cereb. Blood Flow Metab.* **27,** 1941–1953.
29. West, M. J., Slomianka, L., Gundersen, H. J. (1991) Unbiased stereological estimation of the total number of neurons in the subdivisions of the rat hippocampus using the optical fractionator. *Anat. Rec.* **231,** 482–497.
30. Esmann, L., Idel, C., Sarkar, A., Hellberg, L., Behnen, M., Moller, S., van Zandbergen, G., Klinger, M., Kohl, J., Bussmeyer, U., Solbach, W., Laskay, T. (2010) Phagocytosis of apoptotic cells by neutrophil granulocytes: diminished proinflammatory neutrophil functions in the presence of apoptotic cells. *J. Immunol.* **184,** 391–400.
31. Stafslien, D. K., Vedvik, K. L., De Rosier, T., Ozers, M. S. (2007) Analysis of ligand-dependent recruitment of coactivator peptides to RXRβ in a time-resolved fluorescence resonance energy transfer assay. *Mol. Cell. Endocrinol.* **264,** 82–89.
32. Colton, C. A. (2009) Heterogeneity of microglial activation in the innate immune response in the brain. *J. Neuroimmune Pharmacol.* **4,** 399–418.
33. Nakamura, T., Yamamoto, E., Kataoka, K., Yamashita, T., Tokutomi, Y., Dong, Y. F., Matsuba, S., Ogawa, H., Kim-Mitsuyama, S. (2007) Pioglitazone exerts protective effects against stroke in stroke-prone spontaneously hypertensive rats, independently of blood pressure. *Stroke* **38,** 3016–3022.
34. Serhan, C. N., Chiang, N., Van Dyke, T. E. (2008) Resolving inflammation: dual anti-inflammatory and pro-resolution lipid mediators. *Nat. Rev. Immunol.* **8,** 349–361.
35. Ren, Y., Silverstein, R. L., Allen, J., Savill, J. (1995) CD36 gene transfer confers capacity for phagocytosis of cells undergoing apoptosis. *J. Exp. Med.* **181,** 1857–1862.
36. Savill, J., Hogg, N., Ren, Y., Haslett, C. (1992) Thrombospondin cooperates with CD36 and the vitronectin receptor in macrophage recognition of neutrophils undergoing apoptosis. *J. Clin. Invest.* **90,** 1513–1522.
37. Silverstein, R. L., Febbraio, M. (2009) CD36, a scavenger receptor involved in immunity, metabolism, angiogenesis, and behavior. *Sci Signal.* **2,** re3.
38. Serghides, L., Kain, K. C. (2001) Peroxisome proliferator-activated receptor γ-retinoid X receptor agonists increase CD36-dependent phagocytosis of *Plasmodium falciparum*-parasitized erythrocytes and decrease malaria-induced TNF-α secretion by monocytes/macrophages. *J. Immunol.* **166,** 6742–6748.
39. Escribano, L., Simon, A. M., Gimeno, E., Cuadrado-Tejedor, M., Lopez de Maturana, R., Garcia-Osta, A., Ricobaraza, A., Perez-Mediavilla, A., Del Rio, J., Frechilla, D. (2010) Rosiglitazone rescues memory impairment in Alzheimer's transgenic mice: mechanisms involving a reduced amyloid and τ pathology. *Neuropsychopharmacology* **35,** 1593–1604.
40. Yamanaka, M., Ishikawa, T., Griep, A., Axt, D., Kummer, M. P., Heneka, M. T. (2012) PPARγ/RXRα-induced and CD36-mediated microglial amyloid-β phagocytosis results in cognitive improvement in amyloid precursor protein/presenilin 1 mice. *J. Neurosci.* **32,** 17321–17331.
41. Zhao, X., Sun, G., Zhang, J., Strong, R., Song, W., Gonzales, N., Grotta, J. C., Aronowski, J. (2007) Hematoma resolution as a target for intracerebral hemorrhage treatment: role for peroxisome proliferator-activated receptor γ in microglia/macrophages. *Ann. Neurol.* **61,** 352–362.
42. Campanella, M., Sciorati, C., Tarozzo, G., Beltramo, M. (2002) Flow cytometric analysis of inflammatory cells in ischemic rat brain. *Stroke* **33,** 586–592.
43. Carson, M. J., Reilly, C. R., Sutcliffe, J. G., Lo, D. (1998) Mature microglia resemble immature antigen-presenting cells. *Glia* **22,** 72–85.
44. Perego, C., Fumagalli, S., De Simoni, M. G. (2011) Temporal pattern of expression and colocalization of microglia/macrophage phenotype markers following brain ischemic injury in mice. *J. Neuroinflammation* **8,** 174.
45. Cho, S., Park, E. M., Febbraio, M., Anrather, J., Park, L., Racchumi, G., Silverstein, R. L., Iadecola, C. (2005) The class B scavenger receptor CD36 mediates free radical production and tissue injury in cerebral ischemia. *J. Neurosci.* **25,** 2504–2512.
46. Schilling, M., Besselmann, M., Muller, M., Strecker, J. K., Ringelstein, E. B., Kiefer, R. (2005) Predominant phagocytic activity of resident microglia over hematogenous macrophages following transient focal cerebral ischemia: an investigation using green fluorescent protein transgenic bone marrow chimeric mice. *Exp. Neurol.* **196,** 290–297.
47. Hamilton, J. A. (2008) Colony-stimulating factors in inflammation and autoimmunity. *Nat. Rev. Immunol.* **8,** 533–544.
48. Chiang, N., Serhan, C. N., Dahlen, S. E., Drazen, J. M., Hay, D. W., Rovati, G. E., Shimizu, T., Yokomizo, T., Brink, C. (2006) The lipoxin receptor ALX: potent ligand-specific and stereoselective actions in vivo. *Pharmacol. Rev.* **58,** 463–487.
49. Schaldach, C. M., Riby, J., Bjeldanes, L. F. (1999) Lipoxin A4: a new class of ligand for the Ah receptor. *Biochemistry* **38,** 7594–7600.
50. Sato, O., Kuriki, C., Fukui, Y., Motojima, K. (2002) Dual promoter structure of mouse and human fatty acid translocase/CD36 genes and unique transcriptional activation by peroxisome proliferator-activated receptor α and γ ligands. *J. Biol. Chem.* **277,** 15703–15711.
51. Ren, Y., Stuart, L., Lindberg, F. P., Rosenkranz, A. R., Chen, Y., Mayadas, T. N., Savill, J. (2001) Nonphlogistic clearance of late apoptotic neutrophils by macrophages: efficient phagocytosis independent of β 2 integrins. *J. Immunol.* **166,** 4743–4750.
52. Uderhardt, S., Herrmann, M., Oskolkova, O. V., Aschermann, S., Bicker, W., Ipseiz, N., Sarter, K., Frey, B., Rothe, T., Voll, R., Nimmerjahn, F., Bochkov, V. N., Schett, G., Kronke, G. (2012) 12/15-Lipoxygenase orchestrates the clearance of apoptotic cells and maintains immunologic tolerance. *Immunity* **36,** 834–846.

KEY WORDS:
stroke · resolution · lipoxin · microglia · phagocytosis